Bio-Inspired Bimetallic Cooperativity Through a Hydrogen Bonding Spacer in CO 2 Reduction

Chanjuan Zhang, Philipp Gotico, Regis Guillot, Diana Dragoe, Winfried Leibl, Zakaria Halime, Ally Aukauloo

COMMUNICATION

Bio-Inspired Bimetallic Cooperativity Through a Hydrogen Bonding Spacer in CO_2 Reduction

Chanjuan Zhang,[a] Philipp Gotico,[b] Regis Guillot,[a] Diana Dragoe,[a] Winfried Leibl,[b] Zakaria Halime*[a] and Ally Aukauloo*[a, b]

[a] C. Zhang, Dr. R. Guillot, Dr. D. Dragoe, Dr. Z. Halime, Prof. A. Aukauloo
Université Paris-Saclay, CNRS, Institut de Chimie Moléculaire et des Matériaux d'Orsay, 91400, Orsay, France.
E-mail: zakaria.halime@universite-paris-saclay.fr, ally.aukauloo@universite-paris-saclay.fr
[b] Dr. P. Gotico, Dr. W. Leibl, Prof. A. Aukauloo
Institute for Integrative Biology of the Cell, CEA, CNRS, Université Paris-Saclay, 91191, Gif-sur-Yvette, France.

Supporting information for this article is given via a link at the end of the document.

Abstract: At the core of carbon monoxide dehydrogenase (CODH) active site two metal ions together with hydrogen bonding scheme from amino acids orchestrate the interconversion between CO_2 and CO. We have designed a molecular catalyst implementing a bimetallic iron complex with an embarked second coordination sphere with multi-point hydrogen-bonding interactions. We found that, when immobilized on carbon paper electrode, the dinuclear catalyst enhances up to four fold the heterogeneous CO_2 reduction to CO in water with an improved selectivity and stability compared to the mononuclear analogue. Interestingly, quasi-identical catalytic performances are obtained when one of the two iron centers was replaced by a redox inactive Zn metal, questioning the cooperative action of the two metals. Snapshots of X-ray structures indicate that the two metalloporphyrin units tethered by a urea group is a good compromise between rigidity and flexibility to accommodate CO_2 capture, activation, and reduction.

Energy shortages and related environmental problems have raised worldwide concerns. Hence, exploring renewable alternatives to fossil fuels and decreasing carbon dioxide (CO_2) emissions are important challenges ahead of us. In this context, the catalytic conversion of CO_2 into fuels and organic materials using renewable energy sources, either in electrical or light-induced transformation, could provide a virtuous cycle to cut down the accumulation of this greenhouse gas in the atmosphere.[1–8] Among the many catalytic materials currently being investigated to tackle the reduction of CO_2, molecular catalysts containing a series of first-row transition metal catalysts, including N-based macrocyclic and polypyridyl complexes of Mn, Fe, Co and Cu have shown very appealing activity toward CO_2 reduction.[9–19] The ongoing challenges reside in the discovery of highly active cost-efficient performing catalysts. The unique assets of molecular catalysts hinge on the versatile design of ligands sets that can control the electrochemical properties and chemical selectivity of the corresponding metal complexes. In this process, chemists often seek for inspiration from the unmatched reactivity pattern of active sites of metalloenzymes that are involved in essential chemical transformations that sustain life. Notably, one of the interesting shared feature by many substrate-activating enzymes, including those involved in water oxidation,[20] hydrogen evolution,[21] dioxygen reduction[22] and CO_2 reduction,[23] is the presence of a multinuclear active site. At the [NiFe] Carbon Monoxide DeHydrogenase (CODHs) active center, a redox active nickel ion and an iron(II) center acting as a Lewis acid together with a pair of amino acid providing hydrogen bonding,[24,25] manage the reversible interconversion between CO_2 and CO with high efficiency at almost no overpotential.

Only few examples of dinuclear catalysts have been investigated for the photo- or electro-reduction of CO_2.[26–35] Most of these complexes displayed a significant increase of catalytic performances and/or selectivity when compared to their mononuclear analogues, supporting a synergistic action of the two metal centers. However, these systems fail to investigate the differing roles that each metal center plays because of their homometallic nature. Only recently that Duboc and collaborators have developed a more biomimetic [NiFe] heterobimetallic catalyst supported on graphite electrode for the electro-reduction of CO_2.[36] Interestingly, unlike the [NiFe] CODH, a mixture of CH_4 (12 %) and H_2 (66 %) were produced instead of CO.

We have recently developed a highly active series of mononuclear Fe-porphyrin catalysts bearing urea groups in the second coordination sphere as multipoint hydrogen-bonding donors mimicking the amino acid residues in the second sphere of the [NiFe] CODH active site.[37,38] Here, we combine the hydrogen-bonding effects from a urea group with the synergistic effect of two metal centers ([FeFe] for **P_2Ur-FeFe** and [FeZn] for **P_2Ur-FeZn**) in the same catalyst, where two metalloporphyrins are covalently coupled through a urea linker (Figure 1). X-ray structures of these dinuclear catalysts evidenced a good compromise between rigidity and flexibility of the urea linker that can accommodate CO_2 binding and reduction. When immobilized on a carbon paper modified electrode, **P_2Ur-FeFe** displays four times higher catalytic current density with a better CO selectivity than that of **TPP-Fe**. Interestingly, high catalytic performance was also observed when one of the Fe metal centers was replaced by a redox-inactive Zn in **P_2Ur-FeZn**. This provides support to a cooperative action of the two metal centers to activate and reduce CO_2 closely resembling to that proposed in the [NiFe] CODH reaction mechanism.

Catalysts **P_2Ur-FeFe** and **P_2Ur-FeZn** were prepared using a modified version of previously reported procedures and starting from mono-(2-aminophenyl)-tris-(phenyl)-porphyrin.[39] The synthetic procedures (Figure S1 to S3) and characterization (Figures S11 and S23 to S44) of the studied complexes are gathered in the Supplementary Information (SI). X-ray diffraction analyses of **P_2Ur-FeZn** and **P_2Ur-FeFe** were performed on single

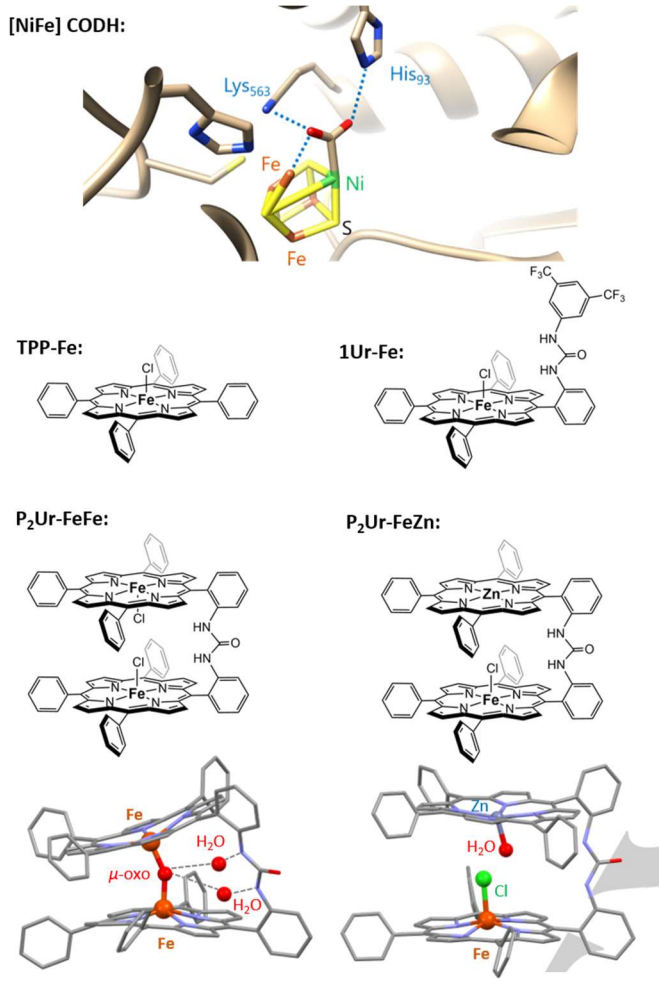

Figure 1. Active site of CO dehydrogenase showing heterobimetallic [NiFe] and hydrogen bonding [Lys, His] activation of CO_2 (Top). Molecular structures of the complexes under investigation (Middle) and their corresponding X-ray crystal structures (bottom).

crystals (Figure 1 and see Table S3 for a more detailed description of the structure). A view of the X-ray structure of **P₂Ur-FeZn** as depicted in Figure 1, presents interesting structural features where a chloride ion as axial ligand on the iron ion and a water bound molecule on the zinc ion are located on the inner space between the porphyrin rings albeit displaced laterally setting the Fe···Zn distance of 5.98 Å. However, the chloride and the oxygen atom of the water molecule are at 2.58 Å indicating a moderate hydrogen bonding interaction.[40] In the case of **P₂Ur-FeFe**, although a chloride (Fe-Cl) derivative was used for the crystallization, the obtained structure shows a *μ*-oxo ligand bridging the two metal ions originating probably from ligand exchange with water and a condensation step. In this case, the Fe···Fe distance of 3.51 Å pertaining the fact that the porphyrin rings can shear to bridge an oxygen atom. Of note the Fe-O-Fe angle of 154.03° is quite severely bent due to the urea linker. The presence of two water molecules inserted between the bridging oxygen atom and the NH groups of the urea function to develop strong hydrogen bonding interactions is also indicative of the presence of a supramolecular pocket in between the porphyrin platforms and the urea function. These structural arrangements set a plausible scenario for a synergistic interaction of the two metal centers, intercalated water molecules and hydrogen bonding interactions toward a CO_2 substrate.

Cyclic voltammograms (CV) of catalyst **P₂Ur-FeFe**, in argon-degassed dimethylformamide (DMF) containing 0.1 M of tetra-*N*-butylammonium hexafluorophosphate ($[Bu_4N]PF_6$), shows three reversible redox waves similar to those recorded for **TPP-Fe** in the same conditions and corresponding to the formal $Fe^{III/II}$, $Fe^{II/I}$, and $Fe^{I/0}$ redox couples (Figure 2 and Table S1). The presence of only three redox waves indicates a weak electronic communication between the two metalloporphyrin units through the urea linker. In the case of **P₂Ur-FeZn**, an extra reduction peak can be observed at –0.986 V *vs* NHE that can be attributed to the first reduction of the Zn-porphyrin unit. The second reduction of this unit occurs at the same potential as that of the formal $Fe^{I/0}$ redox couple with a current intensity corresponding to a two-electron process. Under CO_2 atmosphere and in presence of water (5.5 M) as a proton source, almost identical current intensity corresponding to the catalytic CO_2 reduction was recorded at the last redox wave for the three complexes, *i.e.,* **TPP-Fe**, **P₂UrFeFe** and **P₂Ur-FeZn** when used with a similar Fe-porphyrin unit concentration (Figure 2b). Intriguingly, based on these sets of experiments, no changes in the electrochemical behavior of the bimetallic complexes were detected in comparison with the monometallic complex **TPP-Fe**. As such, suggesting that there is no blatant cooperativity effect between the different metal centers for the CO_2 reduction under the homogeneous catalytic conditions. Reasons behind this could stem from the lack of proximity of the two metal centers in solution or perhaps the protonation of a CO_2 adduct is the rate-determining step in the reaction mechanism as it was previously reported for monometallic iron porphyrins.[37,38,41] Indeed, a kinetic isotope effect (KIE) investigation using H_2O/D_2O as a proton source revealed that for both mononuclear (**TPP-Fe**) and dinuclear (**P₂Ur-FeFe**) catalysts the protonation process is involved in the rate-determining step with respective KIE values of 1.64 and 1.84 (Figure S6 and S9). We then set to interrogate the protonation rate upon increasing the concentration of acid or by using stronger acids. Increasing the proportion of water in DMF indeed increases the reaction rate (Figure S4 and S7). However, due to their hydrophobicity, catalysts **TPP-Fe**, **P₂Ur-FeFe** and **P₂Ur-FeZn** precipitate in the electrolyte at a water content higher than 8 % in DMF before the reaction can reach a catalytic regime where the global reaction rate is no longer dependent on the rate of the protonation process. Replacing water (pK_a = 31.5 in DMF) by stronger acid such as phenol (pK_a = 18.8 in DMF) did not allow either to escape the protonation-controlled reaction regime (Figures S10) and the use of an even stronger acid can result in a loss of selectivity toward CO_2 reduction in favor of proton reduction. With the target to overcome the above limitations we turned to the immobilization of the catalysts at the surface of an electrode. The catalytic ink used in this study was prepared following the typical method of sonicating a mixture containing the iron porphyrin catalyst and multi-walled carbon nanotubes (MWCNTs) in DMF (see SI).[35]

Prior to drop casting the ink on a 1 cm^2 carbon paper electrode, it was first used on a glassy carbon electrode (3 mm diameter) to quickly ensure that the protonation step is no longer the rate-determining step in heterogeneous catalysis. This was confirmed using CV of **TPP-Fe** modified electrode in CO_2-saturated aqueous $KHCO_3$ showing that, unlike in homogeneous catalysis, replacing

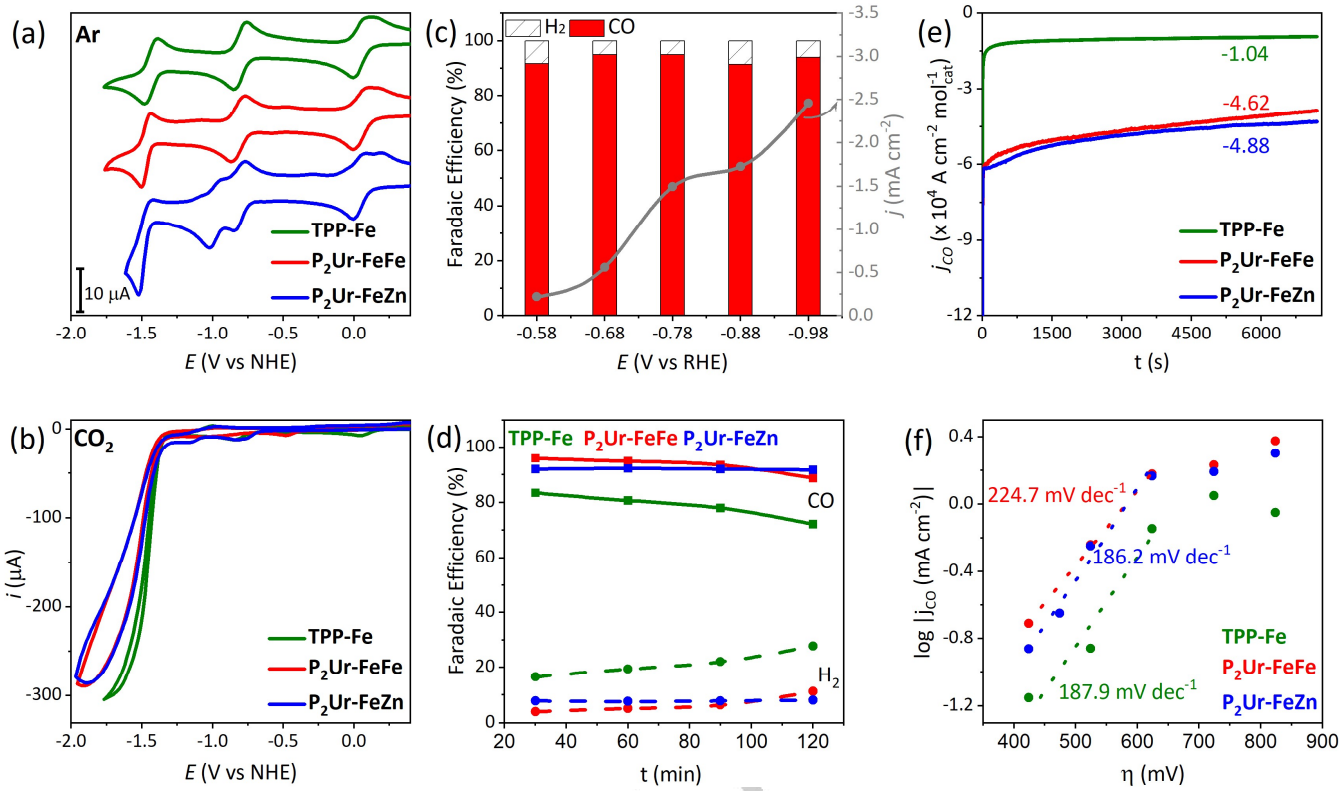

Figure 2. Cyclic voltammograms (CVs) of the complexes **TPP-Fe** (green), **P₂Ur-FeFe** (red) and **P₂Ur-FeZn** (blue) (a) under Ar-saturated homogeneous DMF solution with 0.1 M $[Bu_4N]PF_6$ (b) under CO_2 saturation (bottom) with 5.5 M H_2O. (c) Potential-dependent selectivity and current density of **P₂Ur-FeFe**-modified CNT/CP electrode in CO_2-saturated 0.1 M aqueous $NaHCO_3$ solution. Comparison of (d) Faradaic efficiency, (e) CO partial current density and (f) Tafel plot of heterogenized **TPP-Fe** (green), **P₂Ur-FeFe** (red) and **P₂Ur-FeZn** (blue).

H_2O by D_2O does not induce a significant change in the catalytic current intensity (Figure S13). We found that during the optimization process that a better catalytic efficiency and selectivity for the **P₂Ur-FeFe** could be reached at −0.78 V (Figure 2c and Figure S21) and henceforth all the experiments were performed under the same experimental conditions. In contrast with the homogeneous catalysis, extensive electrolysis for 120 min revealed that, when normalized by the concentration of iron-porphyrin units, the current density displayed by the **P₂Ur-FeFe**-modified electrode is more than four times greater than that of a **TPP-Fe** based electrode (Figure 2e). This result clearly indicates that the electrochemical activity of **P₂Ur-FeFe** for the catalytic CO_2 reduction cannot be accounted for by the sum of two independent iron porphyrins. Furthermore, this result is in sharp contrast with the electrochemical behavior under homogeneous conditions where no apparent change in the current intensity was observed upon electrocatalysis. Gas product analysis also shows that a higher selectivity for CO over the competing H_2-evolution can be maintained for the total duration of the experiment in the case of **P₂Ur-FeFe** (89 %) compared to that of **TPP-Fe** (72 %) (Figure 2d). To evaluate the level of contribution from the urea linker to the catalysis, a mononuclear analogue bearing only one urea arm was also studied (**1Ur-Fe**). Only a slightly higher current density (1.35×10^4 A cm^{-2} mol^{-1}, Figure S15 b and S16) was observed for the **1Ur-Fe**-modified electrode compared to that of **TPP-Fe** (1.04×10^4 A cm^{-2} mol^{-1}). Put together, the observed enhancement of the electrocatalytic activity of **P₂Ur-FeFe** most likely comes from the cooperative effect of the two metal centers. It is worth noting that the concentration of electroactive sites on modified electrodes based on **P₂Ur-FeFe** (r = 2.2 nmol.cm^{-2}) or **TPP-Fe** (r = 2.5 nmol.cm^{-2}) are rather similar (Figure S17 and S18). To further investigate on the conjugated effect of the two metals highlighted by the important enhancement of the catalytic performances of **P₂Ur-FeFe**, one of the iron centers was then replaced by a redox-inactive Zn(II) ion. As a control experiment no catalytic activity toward CO_2 reduction could be observed with a mononuclear **TPP-Zn**-modified electrode (Figure S20), Interestingly, we found that the heterodinuclear **P₂Ur-FeZn** complex, displayed a similar current density and selectivity as **P₂Ur-FeFe** bringing clear support to the participation of both metal centers in the catalytic process but with a differing action of each of the two metal centers. Given that CO is the only two-electron reduced carbon product, with both dinuclear catalysts, it is therefore likely that the adsorption of the catalysts at the surface of the MWCNT does not drastically alter the chemical reactivity. For **P₂Ur-FeFe**, it can be expected that one of the iron-porphyrin to be in direct contact with the MWCNT, acting as the site for electron trade with the electrode while the other iron-porphyrin is not altered electronically.

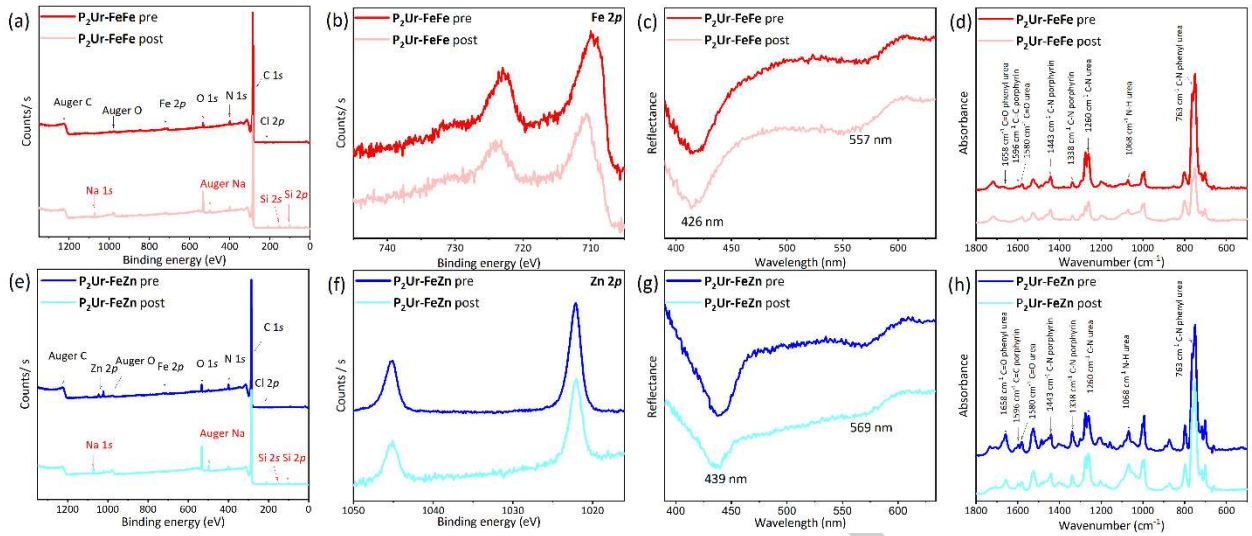

Figure 3. (a, e) XPS survey spectra, (b, f) metal (Fe *2p* or Zn *2p*) high resolution spectra, (c, g) UV-Vis spectra (d, h) ATR-FTIR spectra analyses of the **P_2Ur-FeFe** and **P_2Ur-FeZn** modified CNT/CP electrodes before (red: **P_2Ur-FeFe,** blue: **P_2Ur-FeZn**) and after heterogeneous CO_2 electrolysis (pink: **P_2Ur-FeFe,** cyan: **P_2Ur-FeZn**)

Such a hypothesis can also be transposed to the **P_2Ur-FeZn** catalyst. In this case, two scenarios can be envisioned, *i.e.,* either the iron-porphyrin or the zinc containing porphyrin can be located on the MWCNT, statistically resulting in a lower activity. However, based on the observed slightly higher catalytic performance for **P_2Ur-FeZn**, it seems that a higher catalytic activity of the **P_2Ur-FeZn** compared to **P_2Ur-FeFe** compensate for the statistical drawback. A similar higher activity of a Co-Zn rather than Co-Co dinuclear catalyst for the homogenous photoreduction of CO_2 was also reported by the group of Tong-bu.[42] Hence bringing strong support that both metal ions are working in concert for the two-electron two-proton reduction of CO_2 to CO. Catalytic Tafel analysis shows that, like the mononuclear **TPP-Fe** catalyst, the dinuclear catalysts **P_2Ur-FeFe** and **P_2Ur-FeZn** display also a higher Tafel slop (224.7 and 186.2 mV dec^{-1}, respectively) than that of the theoretical value of 118 mV dec^{-1} observed when the first electron transfer is the rate-determining step (Figure 2f).[43,44] This together with the observation that proton transfer is not the rate determining step under the heterogeneous condition suggest that CO_2 capture or C–O bond cleavage can be the rate-determining step. As discussed earlier, both of these steps can benefit from a cooperative action of two metal centers.

The stability of **P_2Ur-FeFe** and **P_2UrFeZn** modified electrodes was examined using different spectroscopic methods. X-ray photoelectron spectroscopy (XPS) performed on the **P_2Ur-FeFe** modified electrode before and after electrolysis showed similar peaks for C *1s*, N *1s* and Fe *2p* with extra peaks appearing after electrolysis corresponding to Na *1s* and O *1s* coming from $NaHCO_3$ and water in the electrolyte, and Si *2s* and Si *2p* coming from sintered glass in the filters of the electrochemical cell (Figure 3a and 3e). High resolution spectra also show similar N–C=O (urea), C=N and C=C contributions before and after electrolysis (Figure S24a, Table S2), indicating that the electrolysis does not induce a major change in the catalyst structure. Solid state UV-Vis and infrared spectroscopy (FTIR) analysis, also corroborate that the catalyst does not undergo significant structural changes during the electrolysis (Figure 3c and 3d). In the case of a **P_2Ur-FeZn** modified electrode, despite similar UV-Vis and FTIR spectra, some loss of Zn can be evidenced from XPS analysis of the Zn *2p* peaks (Figure 3f and Figure S25) after a long-term electrolysis (> 120 min), due probably to the generally less stable Zn-porphyrin compared to Fe-porphyrin, with only a limited effect on the catalysis performances.

In conclusion, we have synthetized and characterized a family of dinuclear catalyst combining, elements inspired from the CODH active site in that it holds two metal centers in close topology and decorated with a second coordination-sphere hydrogen-bonding interactions from a urea group. Upon immobilization of the dinuclear complexes on carbon paper electrode, we were able to perform the electrocatalytic reduction of CO_2 in water and at a catalytic regime where the cooperativity of the two metal centers are at play. Under these heterogeneous conditions, the **P_2Ur-FeFe**-modified electrode displayed four times greater current density as well as higher selectivity and stability than its **TPP-Fe** analogue. The similar high catalytic performances obtained with the **P_2Ur-FeZn** modified electrode, where an iron center was replaced by a catalytically incompetent and redox-inactive Zn ion, support also a cooperative push/pull activation of the CO_2 resembling the mechanism proposed for the CODH active site. These results set the basis for further investigation in the controlled multi-electronic reduction of CO_2. Efforts are focused on the ligand design to go further than the two-electron reduction of CO_2 in a rational approach.

Acknowledgements

This work has been supported by the French National Research Agency (LOCO, grant N°: ANR-19-CE05-0020-02 and LABEX CHARMMMAT, grant N°: ANR-11-LABX-0039). We thank CNRS, CEA Saclay, ICMMO and University Paris-Saclay for the financial support. We thank the China Scholarship Council for supporting C. Zhang (CSC student number 201904910525). We also thank the analytical support facility at ICMMO for their help with XPS and X-ray diffraction analysis.

Keywords: carbon dioxide • electrocatalysis • bimetallic catalyst • hydrogen bonding • biomimetic

The following contain the supplementary crystallographic data provided free of charge by the Cambridge Crystallographic Data Centre: **P_2Ur-FeFe** (CCDC 2205844), **P_2Ur-FeZn** (CCDC 2205843)

[1] G. A. Olah, *Angew. Chem. Int. Ed.* **2005**, *44*, 2636–2639.
[2] E. E. Benson, C. P. Kubiak, A. J. Sathrum, J. M. Smieja, *Chem. Soc. Rev.* **2008**, *38*, 89–99.
[3] S. Chu, A. Majumdar, *Nature* **2012**, *488*, 294–303.
[4] A. M. Appel, J. E. Bercaw, A. B. Bocarsly, H. Dobbek, D. L. DuBois, M. Dupuis, J. G. Ferry, E. Fujita, R. Hille, P. J. A. Kenis, C. A. Kerfeld, R. H. Morris, C. H. F. Peden, A. R. Portis, S. W. Ragsdale, T. B. Rauchfuss, J. N. H. Reek, L. C. Seefeldt, R. K. Thauer, G. L. Waldrop, *Chem. Rev.* **2013**, *113*, 6621–6658.
[5] M. Aresta, A. Dibenedetto, A. Angelini, *Chem. Rev.* **2014**, *114*, 1709–1742.
[6] Q. Liu, L. Wu, R. Jackstell, M. Beller, *Nat. Commun.* **2015**, *6*, 5933.
[7] T. P. Senftle, E. A. Carter, *Acc. Chem. Res.* **2017**, *50*, 472–475.
[8] O. S. Bushuyev, P. D. Luna, C. T. Dinh, L. Tao, G. Saur, J. van de Lagemaat, S. O. Kelley, E. H. Sargent, *Joule* **2018**, *2*, 825–832.
[9] N. Elgrishi, M. B. Chambers, X. Wang, M. Fontecave, *Chem. Soc. Rev.* **2017**, *46*, 761–796.
[10] A. Rosas-Hernández, C. Steinlechner, H. Junge, M. Beller, *Top. Curr. Chem.* **2017**, *376*, 1.
[11] H. Takeda, C. Cometto, O. Ishitani, M. Robert, *ACS Catal.* **2017**, *7*, 70–88.
[12] F. Wang, *ChemSusChem* **2017**, *10*, 4393–4402.
[13] R. Francke, B. Schille, M. Roemelt, *Chem. Rev.* **2018**, *118*, 4631–4701.
[14] K. E. Dalle, J. Warnan, J. J. Leung, B. Reuillard, I. S. Karmel, E. Reisner, *Chem. Rev.* **2019**, *119*, 2752–2875.
[15] C. Jiang, A. W. Nichols, C. W. Machan, *Dalton Trans.* **2019**, *48*, 9454–9468.
[16] E. Boutin, L. Merakeb, B. Ma, B. Boudy, M. Wang, J. Bonin, E. Anxolabéhère-Mallart, M. Robert, *Chem. Soc. Rev.* **2020**, *49*, 5772–5809.
[17] F. Franco, C. Rettenmaier, H. S. Jeon, B. R. Cuenya, *Chem. Soc. Rev.* **2020**, *49*, 6884–6946.
[18] S. Amanullah, P. Saha, A. Nayek, M. E. Ahmed, A. Dey, *Chem. Soc. Rev.* **2021**, *50*, 3755–3823.
[19] P. Gotico, Z. Halime, A. Aukauloo, *Dalton Trans.* **2020**, *49*, 2381–2396.
[20] W. Lubitz, M. Chrysina, N. Cox, *Photosynth. Res.* **2019**, *142*, 105–125.
[21] W. Lubitz, H. Ogata, O. Rüdiger, E. Reijerse, *Chem. Rev.* **2014**, *114*, 4081–4148.
[22] S. Yoshikawa, K. Shinzawa-Itoh, R. Nakashima, R. Yaono, E. Yamashita, N. Inoue, M. Yao, M. J. Fei, C. P. Libeu, T. Mizushima, H. Yamaguchi, T. Tomizaki, T. Tsukihara, *Science* **1998**, *280*, 1723–1729.
[23] J.-H. Jeoung, B. M. Martins, H. Dobbek, in *Metalloproteins: Methods and Protocols* (Ed.: Y. Hu), Springer, New York, NY, **2019**, pp. 37–54.
[24] H. Dobbek, V. Svetlitchnyi, L. Gremer, R. Huber, O. Meyer, *Science* **2001**, *293*, 1281–1285.
[25] J.-H. Jeoung, H. Dobbek, *Science* **2007**, *318*, 1461.
[26] R. Angamuthu, P. Byers, M. Lutz, A. L. Spek, E. Bouwman, *Science* **2010**, *327*, 313–315.
[27] E. A. Mohamed, Z. N. Zahran, Y. Naruta, *Chem. Commun.* **2015**, *51*, 16900–16903.
[28] A. Taheri, E. J. Thompson, J. C. Fettinger, L. A. Berben, *ACS Catal.* **2015**, *5*, 7140–7151.
[29] C. W. Machan, J. Yin, S. A. Chabolla, M. K. Gilson, C. P. Kubiak, *J. Am. Chem. Soc.* **2016**, *138*, 8184–8193.
[30] T. Ouyang, H.-H. Huang, J.-W. Wang, D.-C. Zhong, T.-B. Lu, *Angew. Chem. Int. Ed.* **2017**, *56*, 738–743.
[31] L.-M. Cao, H.-H. Huang, J.-W. Wang, D.-C. Zhong, T.-B. Lu, *Green Chem.* **2018**, *20*, 798–803.
[32] Z. Guo, G. Chen, C. Cometto, B. Ma, H. Zhao, T. Groizard, L. Chen, H. Fan, W.-L. Man, S.-M. Yiu, K.-C. Lau, T.-C. Lau, M. Robert, *Nat. Catal.* **2019**, *2*, 801–808.
[33] J.-W. Wang, D.-C. Zhong, T.-B. Lu, *Coord. Chem. Rev.* **2018**, *377*, 225–236.
[34] E. A. Mohamed, Z. N. Zahran, Y. Naruta, *J. Mater. Chem. A* **2021**, *9*, 18213–18221.
[35] M. Abdinejad, C. Dao, B. Deng, M. E. Sweeney, F. Dielmann, X. Zhang, H. B. Kraatz, *ChemistrySelect* **2020**, *5*, 979–984.
[36] M. E. Ahmed, S. Adam, D. Saha, J. Fize, V. Artero, A. Dey, C. Duboc, *ACS Energy Lett.* **2020**, 3837–3842.
[37] P. Gotico, B. Boitrel, R. Guillot, M. Sircoglou, A. Quaranta, Z. Halime, W. Leibl, A. Aukauloo, *Angew. Chem. Int. Ed.* **2019**, *58*, 4504–4509.
[38] P. Gotico, L. Roupnel, R. Guillot, M. Sircoglou, W. Leibl, Z. Halime, A. Aukauloo, *Angew. Chem. Int. Ed.* **2020**, *59*, 22451–22455.
[39] J. T. Landrum, D. Grimmett, K. J. Haller, W. R. Scheidt, C. A. Reed, *J. Am. Chem. Soc.* **1981**, *103*, 2640–2650.
[40] T. Steiner, *Angew. Chem. Int. Ed.* **2002**, *41*, 48–76.
[41] C. Costentin, S. Drouet, G. Passard, M. Robert, J.-M. Savéant, *J. Am. Chem. Soc.* **2013**, *135*, 9023–9031.
[42] T. Ouyang, H.-J. Wang, H.-H. Huang, J.-W. Wang, S. Guo, W.-J. Liu, D.-C. Zhong, T.-B. Lu, *Angew. Chem. Int. Ed.* **2018**, *57*, 16480–16485.
[43] X.-M. Hu, M. H. Rønne, S. U. Pedersen, T. Skrydstrup, K. Daasbjerg, *Angew. Chem. Int. Ed.* **2017**, *56*, 6468–6472.
[44] N. Morlanés, K. Takanabe, V. Rodionov, *ACS Catal.* **2016**, *6*, 3092–3095.

Entry for the Table of Contents

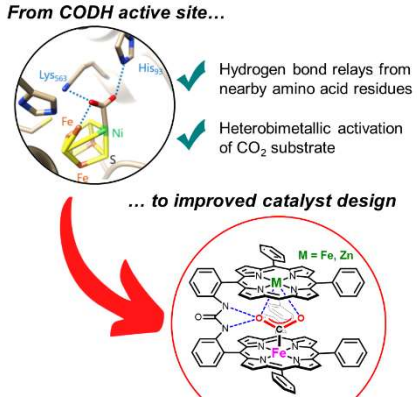

Inspired by the active site of CO dehydrogenase (CODH), a novel metallopoprhyrin-based mimic has been synthesized combining a multipoint hydrogen bond donor and a bimetallic active centre. The cooperativity between the two metal centres of the catalyst was evidenced for both homo- and heterobimetallic analogues leading to a significant enhancement of the catalytic performances of the heterogeneous CO_2-to-CO electrocatalytic reduction in water.